Effect of low-intensity pulsed ultrasound after intraoral vertical ramus osteotomy

Satomi Arimoto, DDS,[a] Takumi Hasegawa, DDS, PhD,[a] Daisuke Takeda, DDS, PhD,[a] Chizu Tateishi, DDS,[a] Masaya Akashi, DDS, PhD,[b] Shungo Furudoi, DDS, PhD,[c] and Takahide Komori, DDS, PhD[d]

Objective. The present study investigated the effect of low-intensity pulsed ultrasound (LIPUS) on long-term osseous healing of the cleavage space between bone fragments after intraoral vertical ramus osteotomy (IVRO).

Study Design. Patients undergoing IVRO were randomly assigned to the LIPUS group (n = 12) or the control group (n = 9) after surgery. LIPUS treatments were applied daily to the cleavage space between bone fragments for 3 weeks. We observed 3-dimensional quantitative color mapping of the whole mandible created by computed tomography (CT) data at 1 month, 6 months, and 1 year postoperatively. On the basis of CT values, the color grades were classified as D1 to D5 by using the Misch criteria. We then calculated mean CT values and rated each color grade in different selection ranges.

Results. The mean CT values of the LIPUS group were significantly higher than those of the control group at 1 month, 6 months and 1 year postoperatively ($P < .01$). The color grades of the cleavage between bone fragments increased from D5 to D1 over time.

Conclusions. Our results indicated that LIPUS promoted osseous healing after IVRO, thus improving bone density and offering clinical benefits. (Oral Surg Oral Med Oral Pathol Oral Radiol 2019;128:581−589)

Many surgical techniques are performed for the treatment of mandibular prognathism. Sagittal split ramus osteotomy and intraoral vertical ramus osteotomy (IVRO) are the most frequently used methods of mandibular ramus osteotomy. Both surgical techniques have risks and benefits. The advantage of IVRO over sagittal split ramus osteotomy is technical simplicity; there is a lower incidence of injury or damage to the inferior alveolar nerve, shorter operation time, and the ability to reposition the condyle.[1] However, IVRO has a prolonged duration of postoperative intermaxillary fixation (IMF) required because of the absence of rigid bone fixation, causing a relatively long interval between the operation and osseous healing. IMF prevents an early return to the usual diet, causes prolonged functional impairment in patients and, when most severe, can compromise the airway during vomiting. Several reports have shown that mandibular prognathism with use of IVRO can be supported by intraoral fixation with a plate or screw instead of IMF.[2] However, it is important to promote osseous healing whether or not IMF is used.

Low-intensity pulsed ultrasound (LIPUS) is known to promote bone healing. In orthopedic surgery, it is a clinically established treatment method used to accelerate long bone fracture healing and is a medical service covered by health insurance in Japan. There has been great interest because of the portability, ease of handling, and noninvasive nature of LIPUS.[3] However, Schandelmaier et al.[4] demonstrated that LIPUS does not improve outcomes that are important to patients and probably has no effect on radiographic bone healing in patients with fresh fractures. However, those authors described that its applicability to other types of fracture or osteotomy is worth considering. We previously demonstrated that cells within mandibular fracture hematomas contribute to mandibular fracture healing and that the osteogenic activity of human mandibular fracture haematoma-derived cells (MHCs) is enhanced by LIPUS stimulation.[5,6] We provided significant evidence for the potential utility of the clinical application of LIPUS to accelerate mandibular fracture healing. Some recent studies have demonstrated the

[a]Clinical Fellow, Department of Oral and Maxillofacial Surgery, Kobe University Graduate School of Medicine, Kusunoki-cho, Chuo-ku, Kobe, Japan.
[b]Assistant Professor, Department of Oral and Maxillofacial Surgery, Kobe University Graduate School of Medicine, Kusunoki-cho, Chuo-ku, Kobe, Japan.
[c]Associate Professor, Department of Oral and Maxillofacial Surgery, Kobe University Graduate School of Medicine, Kusunoki-cho, Chuo-ku, Kobe, Japan.
[d]Professor and Chairman, Department of Oral and Maxillofacial Surgery, Kobe University Graduate School of Medicine, Kusunoki-cho, Chuo-ku, Kobe, Japan.
Received for publication Sep 20, 2018; returned for revision Dec 20, 2018; accepted for publication Mar 9, 2019.

2212-4403/$-see front matter
https://doi.org/10.1016/j.oooo.2019.03.009

Statement of Clinical Relevance

Low-intensity pulsed ultrasound is shown to accelerate mandibular osseous healing in 3 dimensions. It can improve bone density in the cleavage between bone fragments after intraoral vertical ramus osteotomy, with no side effects, thus improving patient outcomes.

significant effect of LIPUS on mandibular defects and fractures.[7-9] However, the therapeutic effect of LIPUS on the healing process after IVRO still remains unclear.

Recently, we demonstrated osseous healing in the cleavage between bone fragments after IVRO by using computed tomography (CT) values in the axial CT images.[10] The CT values between bone fragments significantly increased at 1 month, 6 months, 1 year, and 2 years after surgery. However, radiographic assessment is limited by 2-dimensional interpretations of a 3-dimensional (3-D) structure, and no report so far has investigated the detailed osseous healing of the whole mandible in 3 dimensions. The purpose of this study was to determine the effect of LIPUS on the healing of osteotomy sites after IVRO and observe the long-term osseous healing of the cleavage space between bone fragments after IVRO surgery by using quantitative 3-D analyses of clinical CT data. We hypothesized that LIPUS can accelerate mandibular osseous healing in a manner similar to MHCs reported previously.

Table I. Patient data

				Mandibular setback(mm)	
Case	*Group*	*Age (year)*	*sex*	*Right side*	*Left side*
1	Control	20	M	−8.5	−7
2	Control	40	F	−11	−10.5
3	Control	22	M	−7.5	−5.5
4	Control	20	F	−6	0
5	Control	17	F	−12	−10
6	Control	23	F	−10.5	−1
7	Control	20	M	−6	−8
8	Control	26	F	−5.5	−8.5
9	Control	54	F	−8	3.5
10	LIPUS	18	M	−13	−9
11	LIPUS	33	F	2	−7
12	LIPUS	19	M	−9	−9
13	LIPUS	19	F	−7	−5.5
14	LIPUS	16	F	−8	−8.5
15	LIPUS	21	F	−8	−2
16	LIPUS	19	F	−8.5	−10
17	LIPUS	30	F	−6.5	−5
18	LIPUS	22	M	−9.5	−6
19	LIPUS	19	F	−6.5	−6.5
20	LIPUS	26	F	−7	−6.5
21	LIPUS	21	F	−9	−2.5

F, female; *LIPUS,* low-intensity pulsed ultrasound; *M,* male.

MATERIALS AND METHODS

Ethics

The present study was a prospective cohort study. This study was conducted in full accordance with the tenets of the Declaration of Helsinki. All procedures used in this study were approved by the Ethical Committee of Kobe University Hospital (approval number: No.789), and informed consent was obtained from each patient.

Participants

The inclusion criteria were (1) mandibular prognathism and mandibular set-back surgery with bilateral IVRO, (2) no previous orthognathic surgery and no maxillary surgery, (3) no history of facial fracture or jaw trauma, and (4) availability for all evaluation time points. The exclusion criteria were (1) unwillingness to participate; (2) loss to follow-up at specific time intervals; (3) treatment with steroids, anticoagulants, prescription nonsteroidal anti-inflammatory medication, calcium-channel blockers, or diphosphonate therapy; (4) a history of thrombophlebitis, vascular insufficiency, or a recent history of alcoholism or nutritional deficiency.[11]

In total, 21 patients (6 males and 15 females) were randomly selected from mandibular prognathism cases of patients who underwent bilateral IVRO (42 rami) at our institution between August 2007 and March 2014. The operations were performed by 2 surgeons with a minimum of 20 years of surgical experience in oral and maxillofacial surgery. Patients were then randomly allocated to be treated with LIPUS (12 osteotomies, LIPUS group) or without LIPUS (9 osteotomies, control group) after surgery (Table I). At the beginning of the study, the first patient to be accepted was assigned to the active treatment group. Other patients were assigned to the placebo group or treatment group in an alternating order. The patients' ages ranged from 16 to 54 years (mean age 24.0 ± 1.9 years). The mean setback was 6.8 ± 0.4 mm. There was no potential impact of age, sex, and mandibular setback on the present study. All patients underwent IMF with stainless steel wires (0.3 mm), and brackets were placed in the maxillary and mandibular arches for 14 days, according to the established clinical pathway.

LIPUS treatment

Ultrasonography was performed with the Sonic Accelerated Fracture Healing System 2000 (SAFHS; Teijin Pharma, Tokyo, Japan). Starting 2 days postoperatively, patients in the LIPUS group received one 20-minute LIPUS treatment per day for 3 weeks (intensity: 30 mW/cm^2; burst width: 200 μs; frequency: 1.5 MHz). The transducer was located on the angle of the mandibular ramus at the level of the osteotomy and was firmly fixed with a facial bandage (Figure 1). Coupling gel was used to ensure effective transfer of the acoustic wave to the tissue. After being properly trained on the correct positioning of the device, the study patients self-administered the LIPUS treatment. The use of the LIPUS machine was checked every day while the patients were in the hospital for 3 weeks.

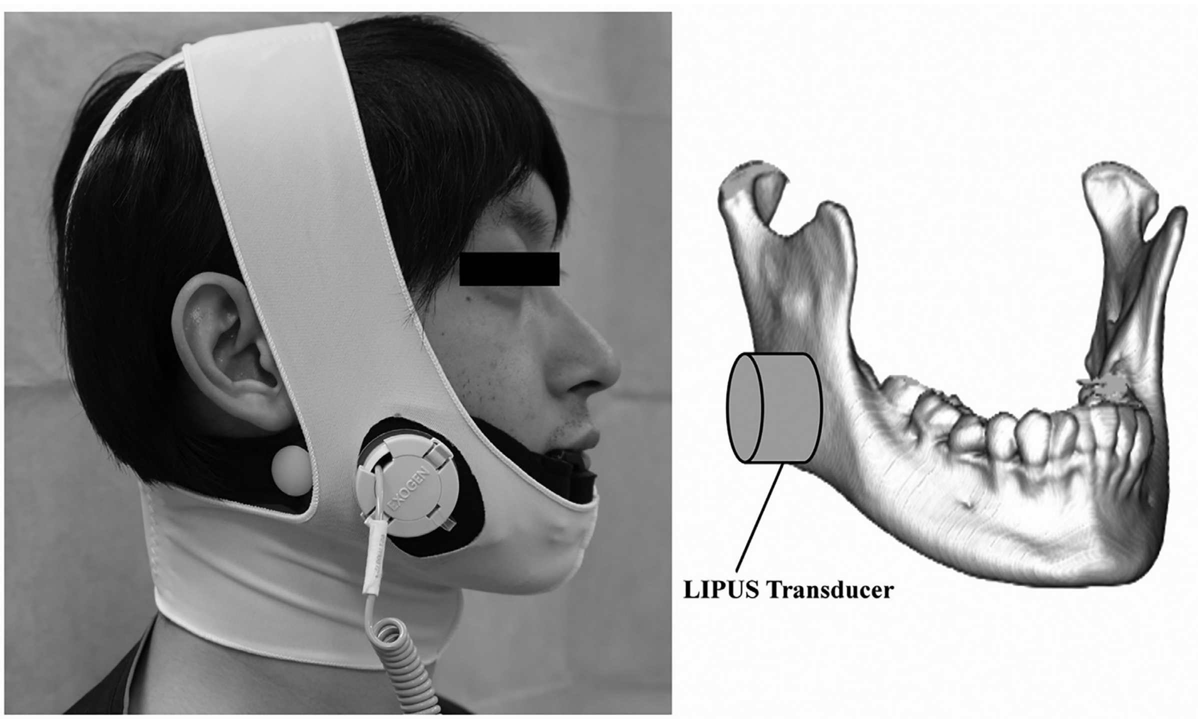

Fig. 1. Position of the low-intensity pulsed ultrasound (LIPUS) transducer. The LIPUS transducer was located on the angle of the mandibular ramus at the level of the osteotomy and was firmly fixed with a facial bandage. Coupling gel was used to ensure effective transfer of the acoustic wave to the tissue.

CT measurement procedure

CT examinations were performed in all patients at 1 month, 6 months, and 1 year postoperatively with Aquilion64 (Toshiba Medical Systems, Tokyo, Japan) at the Wakaba Imaging Support Center (tube current: 100 mA; scanning time: 3 seconds; slice thickness: 2 mm; slice width: 2 mm; field of view: 25 cm). The slice plane was parallel to the occlusal plane, and the scanned area extended from the floor of the orbit to the inferior border of the mandible. To reduce the data variation, a single author (S.A.) measured all of the CT images in this study. This person was blinded with regard to the treatment received and assessed all CT images obtained from each patient. The raw data was transferred to a dedicated workstation (Ziostation2 ver.2.1.5.0; Ziosoft, Tokyo, Japan) with technical consultation. Based on the Ueki visualization method,[12] the frontozygomatic line was defined as the line connecting the most lateral points of the bilateral frontozygomatic sutures in the coronal CT images (Figures 2A and 2C). The right and left side lines were defined as the lines connecting the most anterior points of the bilateral auricles in the axial CT images (Figure 2B). Kim et al.[13] reported that the color maps created from CT images reconstructed with a section width of 2 mm had better image quality and retained more anatomic details compared with those reconstructed with a section width of 3 mm. Therefore, 3-D volumes were reconstructed with slice imaging with multiplanar reconstruction by using a section width of 2 mm as described in Figures 2A−2C. All slices were quantified, and bone fragment healing methods were clarified. On the axial CT images, we drew a line tangent to the bilateral foramen−mandibular posterior region to separate the posterior areas (Figure 2D). With regard to the coronal CT images, we extracted only the part of the mandibular bone that contained the cleavage (Figure 2E). On the basis of the Hagino visualization method,[14] we determined reference points of Porion (Po) and crest of articular eminence (CAE) on the sagittal CT images. We drew a line perpendicular to the Po−CAE line, starting from the top of the coronoid process in the sagittal images to separate the CT values of the mandible bone from those of wisdom teeth (Figure 2F). Each analysis volume was divided into 2 sections of CT slices. On the axial CT images, the upper half of CT slices were defined as the "upper side" of the CT slices, and the "lower side" was defined as the lower half of CT slices. Similarly, for the other directions of the 3-D volume, on the sagittal and coronal CT images, half the CT slices were defined as the "interior side," and the other half were defined as the "lateral side." The "anterior side" and the "posterior side" were defined, respectively, with the halves of the CT slices taken.

CT can be used to obtain the desired information about morphologic changes, and the linear attenuation coefficient of bone density is measured in Hounsfield

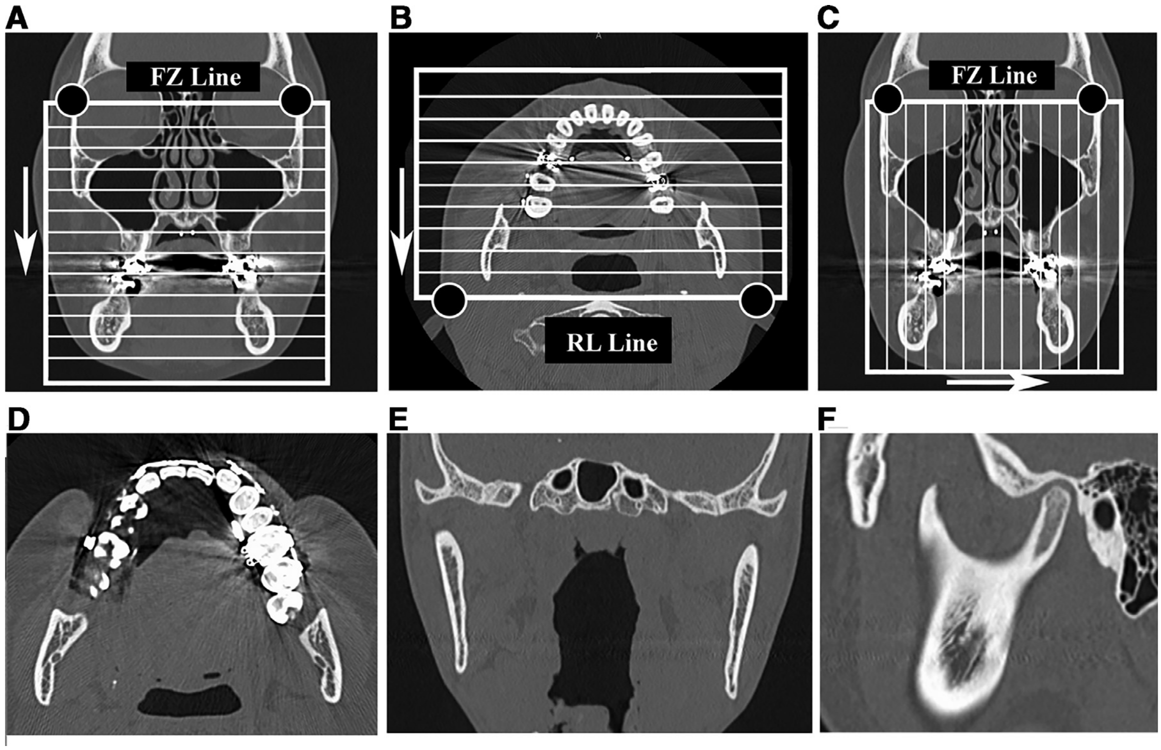

Fig. 2. Method of measuring 3-dimensional quantitative color mapping created by using computed tomography (CT) data. The frontozygomatic line (FZ line) was defined as the line between the most lateral points of the bilateral frontozygomatic sutures **(A,C)**.The right and left side lines (RL line) was defined as the line between the most anterior points of the bilateral auricles **(B)**. **A-C,** On the basis of the reference point, 3-dimensional data were reconstructed with 2-mm-width slice imaging by multiplanar reconstruction. **(D)** We drew a line tangent to the bilateral foramen−mandibular posterior region and measured the posterior areas. **(E)** We extracted only the part of the mandibular bone that contained the cleavage. **(F)** We determined reference points of Porion (Po), crest of articular eminence (CAE). We drew the vertical line of Po−CAE line, which passed through the top of the coronoid process and measured the posterior areas.

units (HU). The CT values are correlated with bone quality.[15] Misch categorized bone quality as D1 to D5, based on HU values.[16] Rokn et al. reported that the Misch criteria can characterize the histologic properties of bone.[17] In the present study, the long-term osseous healing of the cleavage space between bone fragments was shown by color maps coded with CT values in HU. The color grades were classified into 5 categories by using the CT values as follows: greater than 1250 HU, red (D1); 850 to 1250 HU, yellow (D2); 350 to 849 HU, green (D3); 150 to 349 HU, blue (D4); and less than 150 HU, black (D5) (Figure 3A). D1 bone is primarily dense cortical bone; D2 bone has dense and thick porous cortical bone on the crest and coarse trabecular bone underneath; D3 bone has thinner porous cortical crest and fine trabecular bone within; and D4 has almost no crestal cortical bone, with fine trabecular bone comprising almost all of the total volume of bone. The warm colors represent the cortical bone areas with high CT values, whereas the cold colors represent the trabecular bone and the soft tissue areas with low CT values. We measured the mean CT values and rated each color grade in the selection range.

Misch criteria

grade	color	CT values(HU)
D1		>1250
D2		850-1250
D3		350-849
D4		150-349
D5		150>

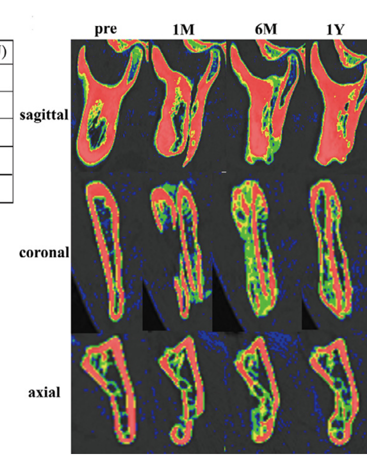

Fig. 3. Classification of 5 color grades. **(A)** On the basis of the Misch criteria, the color grades were classified into 5 steps using the CT values. **(B)** The color grades of the cleavage between bone fragments increased from D5 to D1 over time.

Statistical analysis

The data collection and statistical analyses were performed by using Statistical Package for the Social Sciences for Windows version 22.0 (SPSS Inc., Chicago, IL). Data were presented as mean ± standard deviation. The Mann-Whitney U test was used to assess the differences in the means between the control and LIPUS groups at each time point. A value of $P < .05$ was considered statistically significant.

RESULTS

During the present study, no adverse events occurred in either group of patients. We successfully demonstrated the visualization of the cleavage between healing bone fragments. The color grades of the cleavage between bone fragments increased from D5 to D1 over time (Figure 3B).

There were no significant differences between the control and LIPUS groups in age, sex, or mandibular setback. On the sagittal CT images, the mean CT values of the control group were 1054 ± 18 HU preoperatively; 915 ± 20 HU at 1 month; 916 ± 20 HU at 6 months; and 952 ± 21 HU at 1 year. The LIPUS group's values were 1012 ± 13 HU preoperatively; 994 ± 8 HU at 1 month; 1011 ± 7 HU at 6 months; and 1049 ± 12 HU at 1 year. On the sagittal CT images, the LIPUS group's CT values were significantly higher than those of the control group at 1 month ($P < .05$), 6 months, and 1 year ($P < .01$) postoperatively (Figure 4A). On the axial CT images, the mean CT values of the control group were 1006 ± 17 HU preoperatively; 856 ± 18 HU at 1 month; 880 ± 22 HU at 6 months; and 909 ± 25 HU at 1 year. The LIPUS group's CT values were 985 ± 15 HU preoperatively; 923 ± 8 HU at 1 month; 955 ± 10 HU at 6 months; and 1002 ± 12 HU at 1 year. On the axial CT images, the LIPUS group had significantly higher CT values compared with the control group at 1 month, 6 months, and 1 year ($P < .01$) postoperatively (Figure 4B). On the coronal CT images, the mean CT values of the control group were 1002 ± 20 HU preoperatively; 862 ± 19 HU at 1 month; 862 ± 22 HU at 6 months; and 878 ± 21 HU at 1 year. The LIPUS group had values of 1003 ± 16 HU preoperatively; 924 ± 10 HU at 1 month; 930 ± 13 HU at 6 months; and 963 ± 18 HU at 1 year (Figure 4C). On the axial CT images and coronal CT images, the mean CT value of the LIPUS group was significantly higher than those of the control group at 1 month, 6 months, and 1 year ($P < .01$) postoperatively. There were no significant differences among all images at the preoperative time point.

The posterior side of the coronal color-mapped CT images showed a significantly higher amount of D1 grade area in the LIPUS group compared with the control group at 6 months ($P < .05$) and 1 year ($P < .01$) postoperatively (Figure 5A). As well, the amount of D4 grade area of the control group was significantly higher than that of the LIPUS group at 1 year ($P < .05$) postoperatively. The anterior side of the images showed a higher amount of D1 grade area in the LIPUS group compared with the control group at 1 year ($P < .05$) postoperatively (Figure 5B). On the lower side of the axial color-mapped CT images, the amount of D1 and D2 grade areas of the LIPUS group were significantly higher than those of the control group at 1 month ($P < .01$ for D1 grade), 6 months ($P < .05$ for D1 and D2 grade areas), and 1 year ($P < .01$ for D1 grade; $P < .05$ for D2 grade) postoperatively (Figure 5C). On the upper side of the

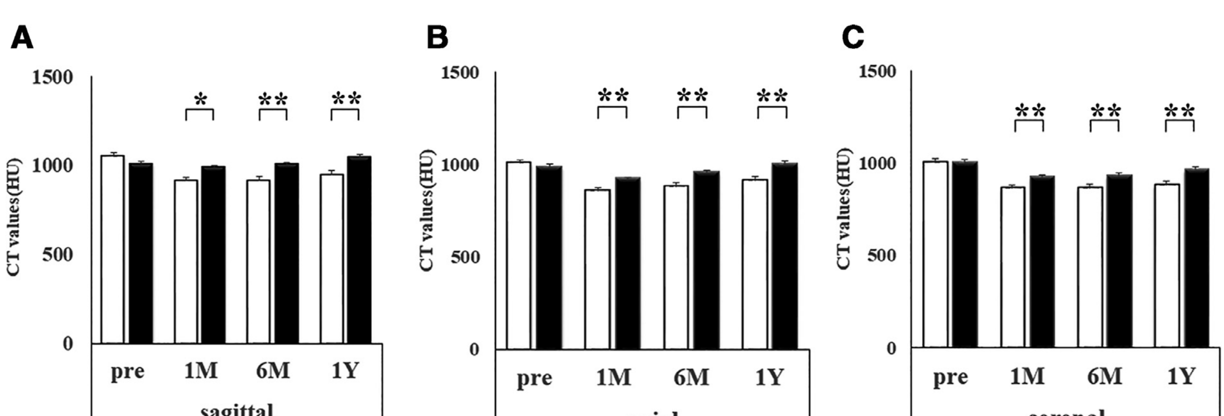

	pre	1M	6M	1Y
□Control	1054±18	915±20	916±20	952±21
■LIPUS	1012±13	994±8	1011±7	1049±12

	pre	1M	6M	1Y
□Control	1006±17	856±18	880±22	909±25
■LIPUS	985±15	923±8	955±10	1002±12

	pre	1M	6M	1Y
□Control	1002±20	862±19	862±22	878±21
■LIPUS	1003±16	924±10	930±13	963±18

* P <0.05 ** P <0.01

Fig. 4. Mean computed tomography (CT) values ± standard deviation in the sagittal images **(A)** the axial images **(B)** and coronal images **(C)**.

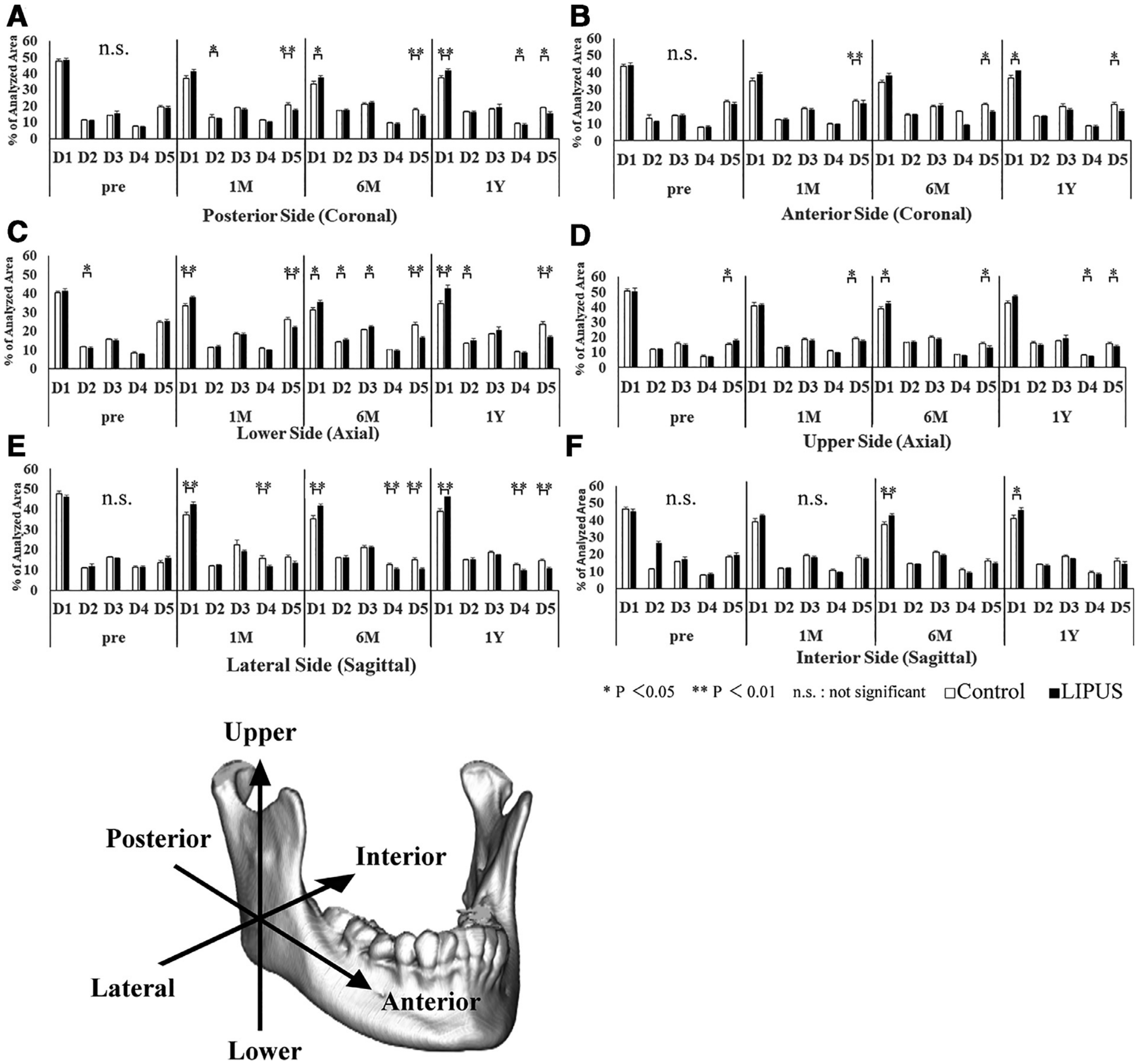

Fig. 5. **(A−F)** Rating of each color grade in the divided 2 sections of all slices. Percent of area covered by each bone grade in the divided 2 sections of all slices.

images, the amount of D1 grade area of the LIPUS group was significantly higher than that of the control group at 6 months ($P < .05$) postoperatively (Figure 5D). On the lateral side of the sagittal color-mapped CT images, the amount of D1 grade area of the LIPUS group was significantly higher than that of the control group at 1 month, 5 months, and 1 year ($P < .01$) postoperatively (Figure 5E). The amount of D4 grade area of the control group was significantly higher than that of the LIPUS group at 1 month, 6 months, and 1 year ($P < .01$) postoperatively. On the interior side, the amount of D1 grade area of the LIPUS group was significantly higher than that of the control group at 6 months ($P < .01$) and 1 year ($P < 0.05$) postoperatively (Figure 5F). There were no significant differences at 1 month.

DISCUSSION

We successfully demonstrated osseous healing in the cleavage between bone fragments after IVRO by using quantitative 3-D analysis of clinical CT data. The results suggested that LIPUS can increase bone density, thus offering clinical benefits.

Quantitative color mapping of CT offers a wide range of applications in the medical and dental fields. Recently, it has been used for the evaluation of the arterial enhancement fraction of the liver,[18,19] diagnosis of coronary artery disease,[20] prediction of intra-ascending aorta,[21] and analysis of bone properties in hip osteoarthritis.[22] Meyer et al.[23] provided evidence that assessing the degree and location of the osseointegration of dental implants is valid with the use of quantitative color mapping of the CT.

Buchtala[24] was the first to report the possibility of stimulating osteogenesis with ultrasound in 1950. Since then, LIPUS has demonstrated enhanced fracture healing in animal studies and bone repair in humans. It has shown a positive effect on accelerating bone healing of fresh fractures, with highly significant evidence in experimental and double-blind, randomized, placebo-controlled studies.[11,25] The advantages of this technology are its efficacy, safety, and ease of use. In the United States, the Food and Drug Administration approved the use of LIPUS in October 1994 for accelerating healing of fresh fractures and in February 2000 for the treatment of established nonunions. Erdogan et al.[7] reported that LIPUS improved the bone healing of mandibular fractures in rabbits. In their study, LIPUS treatment was administered for 20 minutes daily for 20 days, with an ultrasound signal consisting of 1.5 MHz pressure wave administered in pulses of 200 μs with an average temporal and spatial intensity of 30 mW/cm^2. We utilized this waveform in our previous study[5,6] and demonstrated that human mandibular fracture hematoma−derived cells play an important role in mandibular fracture healing and that LIPUS accelerates this effect by stimulating various osteogenic cytokines. The gene expression levels of alkaline phosphatase, osteocalcin, bone morphogenetic proteins 2, 4, and 7, runt-related gene 2 (*Runx2*), osterix, osteopontin, parathyroid hormone receptor 1, and mineralization were increased in the LIPUS (+) group compared with the LIPUS (−) group (control). Histologic studies proved that LIPUS influences osteoblasts, osteoclasts, chondrocytes, and mesenchymal stem cells in bone healing. This evidence was used to select the waveform properties in the present study. Patel et al.[8] demonstrated significant improvement in the healing rate of mandibular fractures as shown by radiographic density findings and significant, rapid reduction in pain perception in the LIPUS group compared with the control group. Uchida et al.[26] showed that LIPUS stimulated vascular endothelium growth factor expression in their experiment by using the femoral fracture model of mice. Young et al.[27] showed increased angiogenesis in the form of increased blood vessel formation after the application of LIPUS. Rawool et al.[28] demonstrated that LIPUS increased blood flow around the fracture and surrounding tissue by using Power Doppler imaging for the first 2 weeks after surgery. In the present study, patients in the LIPUS group received daily LIPUS treatments for at least 3 weeks postoperatively. The mean CT values of the LIPUS group were significantly higher than those of the control group at 1 month ($P < .05$), 6 months, and 1 year ($P < .01$) postoperatively. Considering the results, it could be hypothesized that the increase in blood flow produced an increase in cellular calcium uptake, resulting in increased protein synthesis, thereby accelerating osseous healing.

In many other studies, the LIPUS transducer is usually placed transcutaneously during clinical treatments, hence fractures of superficial bone and deeper bone fractures at different depths are exposed to the ultrasound beam at different axial distances. Studies have observed near-field LIPUS on fractures or cells cultures; Reher et al.[29] found that near-field LIPUS at an axial distance of 5 mm could stimulate bone formation. Fung et al.[30] applied LIPUS at 3 different axial distance fields to rats with femoral fractures and observed that LIPUS augmented the callus bone volume and mineralization in the far field (130 mm) and enhanced woven bone formation in the near field (0 mm) and mid-near field (60 mm). Similarly, we found that the increase in the D1 grade area on the posterior side was faster compared with that of the anterior side on coronal images. Furthermore, the lower side was faster than the upper side in the axial images, and the lateral side was faster than the interior side on the sagittal images. These results may have resulted from differences in the distance from the LIPUS transducer areas further away from the LIPUS application site, yielding slower healing. In our study, we found that LIPUS can accelerate osseous healing in 3 dimensions in both near-field and far-field areas.

In fracture healing, the periosteum is the main source for the repair of cells and mainly contributes to callus formation. Ozaki et al.[31] reported that the periosteum is important for mediating in fracture healing. Tam et al.[32] demonstrated the positive stimulatory effect of LIPUS on human periosteal cell culture in the functional activation of bone formation and cellular differentiation. Previously, we observed the long-term osseous healing of the cleavage space between bone fragments after IVRO surgery on the interior and lateral sides.[10] In that study, LIPUS was not applied, hence the recovery of the CT values on the lateral side was less than that observed on the interior side at 2 years postoperatively. In the procedure adopted at our institution, the periosteum of the lateral side of the mandible is elevated and not removed, whereas the interior side is neither elevated nor removed. We reported that the blood supply from the interior side periosteum may affect the speed of osseous healing. In the present study, we observed that on the lateral side, the amount of D1 grade area in the LIPUS group was significantly higher than that of the control group at 1 month, 6 months, and 1 year postoperatively ($P < .01$). Considering these results, we hypothesized that LIPUS stimulated the periosteal bone formation of the lateral side of the mandible. Leung et al.[33] found that the stimulatory effect lasted much longer after LIPUS treatment. They reasoned that the level of plasma bone-specific alkaline phosphatase activity remained persistently higher at weeks 12, 18, and 27. Those authors, therefore, reported that the number of bone-forming cells increased in the early phase and that the activity lasted much longer in the treatment group. Similar results were obtained in the present study.

Our study has some limitations. First, our sample size was small, so further studies with a bigger sample size are required to confirm the results of this study. Second, the range of patient ages was large. Although the study patients did not have a history of osteopenia or osteoporosis, we did not measure bone mineral density preoperatively. It is possible that there may be a potential risk. Third, although LIPUS can improve bone density, the period of the postoperative IMF remains uncertain and should be studied more in depth. Finally, we did not use a sham device in the control group. We could have applied such a device to patients to constitute a stronger placebo group. Further consideration of this will be needed to draw additional implications. We plan to continue to quantitatively evaluate the process of osseous healing.

CONCLUSIONS

The results observed in this study suggest that LIPUS can improve bone density, thus offering clinical benefits. We identified no side effects related to LIPUS treatment. In addition, patients felt no discomfort during therapy. The purpose of this study was to observe long-term osseous healing by using quantitative 3-D analysis of clinical CT data, which successfully demonstrated detailed osseous healing of the mandible bone in 3 dimensions. We believe that our findings will contribute to the successful treatment of patients with the use of IVRO in the fields of dentistry and oral surgery.

ACKNOWLEDGMENTS

We thank all of our colleagues in the Department of Oral and Maxillofacial Surgery. We are particularly grateful for the assistance given by Kaito Uryu. We would also like to express our gratitude to our families for their moral support and warm encouragement.

REFERENCES

1. Pan JH, Lee JJ, Lin HY, et al. Transverse and sagittal angulations of proximal segment after sagittal split and vertical ramus osteotomies and their influence on the stability of distal segment. *J Formos Med Assoc*. 2013;112:244-252.
2. Hara S, Mitsugi M, Tatemoto Y. Variation of plate fixation for mandibular advancement with intraoral vertical ramus osteotomy using endoscopically assisted intraoral rigid or semi-rigid internal fixation: case series study: postoperative condylar seating control for mandibular advancement. *J Craniomaxillofac Surg*. 2015;43:2012-2016.
3. Pomini KT, Andreo JC, Rodrigues Ade C, et al. Effect of low-intensity pulsed ultrasound on bone regeneration: biochemical and radiologic analyses. *J Ultrasound Med*. 2014;33:713-717.
4. Schandelmaier S, Kaushal A, Lytvyn L, et al. Low intensity pulsed ultrasound for bone healing: systematic review of randomized controlled trials. *BMJ*. 2017;356:j656. 22.
5. Huang W, Hasegawa T, Imai Y, Takeda D, Akashi M, Komori T. Low-intensity pulsed ultrasound enhances bone morphogenetic protein expression of human mandibular fracture haematoma-derived cells. *Int J Oral Maxillofac Surg*. 2015;44:929-935.
6. Imai Y, Hasegawa T, Takeda D, et al. The osteogenic activity of human mandibular fracture haematoma-derived cells is stimulated by low-intensity pulsed ultrasound in vitro. *Int J Oral Maxillofac Surg*. 2014;43:367-372.
7. Erdogan O, Esen E, Ustün Y, et al. Effects of low-intensity pulsed ultrasound on healing of mandibular fractures: an experimental study in rabbits. *J Oral Maxillofac Surg*. 2006;64:180-188.
8. Patel K, Kumar S, Kathiriya N, et al. An evaluation of the effect of therapeutic ultrasound on healing of mandibular fracture. *Craniomaxillofac Trauma Reconstr*. 2015;8:299-306.
9. Schortinghuis J, Ruben JL, Raghoebar GM, Stegenga B. Ultrasound to stimulate mandibular bone defect healing: a placebo-controlled single-blind study in rats. *J Oral Maxillofac Surg*. 2004;62:194-201.
10. Arimoto S, Hasegawa T, Kaneko K, et al. Observation of osseous healing after intraoral vertical ramus osteotomy: focus on computed tomography values. *J Oral Maxillofac Surg*. 2013;71:1602. e1-1602. e10.
11. Heckman JD, Ryaby JP, McCabe J, Frey JJ, Kilcoyne RF. Acceleration of tibial fracture-healing by noninvasive, low-intensity pulsed ultrasound. *J Bone Joint Surg*. 1994;76:26-34.
12. Ueki K, Hashiba Y, Marukawa K, et al. The effects of changing position and angle of the proximal segment after intraoral vertical ramusosteotomy. *Int J Oral Maxillofac Surg*. 2009;38:1041-1047.
13. Kim KW, Lee JM, Klotz E, et al. Quantitative CT color mapping of the arterial enhancement fraction of the liver to detect hepatocellular carcinoma. *Radiology*. 2009;250:425-434.
14. Hagino H, Sawaki Y, Oda T, et al. Clinical study of intraoral−vertical ramus osteotomy—Part.1 Radiologic Study of Proximal Segments. *J Jaw Deform*. 1996;6:32-40.
15. Wyatt CCL, Pharoah MJ. Imaging techniques and image interpretation for dental implant treatment. *Int J Prosthodont*. 1998;11:442-452.
16. Misch CE. Density of bone: effect on treatment plans, surgical approach, healing and progressive bone loading. *Int J Oral Implantol*. 1990;6:23-31.
17. Rokn AR, Labibzadeh A, Ghohroudi AAR, Shamshiri AR, Solhjoo S. Histomorphometric analysis of bone density in relation to tactile sense of the surgeon during dental implant placement. *Open Dent J*. 2018;12:46-52. 31.
18. Park M, Chung YE, Kim KA, et al. Added value of arterial enhancement fraction color maps for the characterization of small hepatic low-attenuating lesions in patients with colorectal cancer. *PLoS One*. 2015;10:e0114819. 23.
19. Mahnken AH, Klotz E, Schreiber S, et al. Volumetric arterial enhancement fraction predicts tumor recurrence after hepatic radiofrequency ablation of liver metastases: initial results. *AJR Am J Roentgenol*. 2011;196:W573-W579.
20. Wang Q, Qin J, Gai LY, et al. A pilot study on diagnosis of coronary artery disease using computed tomography first-pass myocardial perfusion imaging at rest. *J Zhejiang Univ Sci B*. 2011;12:485-491.
21. Zhang Q, Xu R, Sun Q, et al. Exploring the value of using color-coded quantitative DSA evaluation on bilateral common carotid arteries in predicting the reliability of intra-ascending aorta flat

detector CT-CBV maps. *AJNR Am J Neuroradiol*. 2015;36: 960-966.
22. Turmezei TD, Treece GM, Gee AH, Fotiadou AF, Poole KE. Quantitative 3-D analysis of bone in hip osteoarthritis using clinical computed tomography. *Eur Radiol*. 2016;26:2047-2054.
23. Meyer J, Sheets CG, Earthman JC. Visualization of osseointegration of maxilla and mandible dental implants. *Int J Comput Assist Radiol Surg*. 2010;5:69-76.
24. Buchtala V. Present state of ultrasound therapy. *Dia Med*. 1950;22:2944-2950.
25. Kristiansen TK, Ryaby JP, McCabe J, Frey JJ, Roe LR. Accelerated healing of distal radial fractures with the use of specific, low-intensity ultrasound. A multicenter, prospective, randomized, double-blind, placebo-controlled study. *J Bone Joint Surg Am*. 1997;79:961-973.
26. Uchida K, Urabe K, Naruse K, et al. Accelerated fracture healing targeting periosteal cells: possibility of combined therapy of low-intensity pulsed ultrasound (LIPUS), bone graft, and growth factor (bFGF). *J Orthop Trauma*. 2016;30:S3.
27. Young SR, Dyson M. The effect of therapeutic ultrasound on angiogenesis. *Ultrasound Med Biol*. 1990;16:261-269.
28. Rawool NM, Goldberg BB, Forsberg F, Winder AA, Hume E. Power Doppler assessment of vascular changes during fracture treatment with low-intensity ultrasound. *J Ultrasound Med*. 2003;22:145-153.
29. Reher P, Elbeshir el-NI, Harvey W, Meghji S, Harris M. The stimulation of bone formation in vitro by therapeutic ultrasound. *Ultrasound Med Biol*. 1997;23:1251-1258.
30. Fung CH, Cheung WH, Pounder NM, de Ana FJ, Harrison A, Leung KS. Investigation of rat bone fracture healing using pulsed 1.5 MHz, 30 mW/cm(2) burst ultrasound—axial distance dependency. *Ultrasonics*. 2014;54:850-859.
31. Ozaki A, Tsunoda M, Kinoshita S, Saura R. Role of fracture hematoma and periosteum during fracture healing in rats: interaction of fracture hematoma and the periosteum in the initial step of the healing process. *J Orthop Sci*. 2000;5:64-70.
32. Tam KF, Cheung WH, Lee KM, Qin L, Leung KS. Osteogenic effects of low-intensity pulsed ultrasound, extracorporeal shockwaves and their combination—an in vitro comparative study on human periosteal cells. *Ultrasound Med Biol*. 2008;34: 1957-1965.
33. Leung KS, Lee WS, Tsui HF, Liu PP, Cheung WH. Complex tibial fracture outcomes following treatment with low-intensity pulsed ultrasound. *Ultrasound Med Biol*. 2004;30:389-395.

Reprint requests:

Takumi Hasegawa
Department of Oral and Maxillofacial Surgery
Kobe University Graduate School of Medicine
7-5-1, Kusunoki-cho
Chuo-ku
Kobe 650-0017
Japan.
Hasetaku@med.kobe-u.ac.jp